Development of new high temperature metallic coating materials

Q. Mohsen

Materials and Corrosion Group, Department of Chemistry, Taif University, Saudi Arabia
mohsen9907@hotmail.com

Abstract: Flaring natural gas is a routine practice in the course of oil production. This study presents two parts. The first one is presenting analyses of corrosion damage experienced by a plasma-sprayed coating of SS310 alloy, after exposure to a simulated flare tip environment at 975 ^{o}C. Samples made of SS310 were utilized to evaluate a proposed coating system, which consists of top coat with yttria stabilized zirconia and a bond coat of Co32Ni21Cr8Al0Y. A simulated gas composition of a flare tip environment was suggested as; CO_2 5%: SO_2 9.58%: H_2O 3.59%: N_2 81.83%. The second part of this study is focused on a practical methodology for synthesis $SrA1_{l2}O_{19}$ as promising material for high temperature thermal barrier coating (TBC) through simple self combustion (organic acid thermal dissociation) routes.
[Q. Mohsen. **Development of new high temperature metallic coating materials.** *J Am Sci* 2018;14(7):65-70]. ISSN 1545-1003 (print); ISSN 2375-7264 (online). http://www.jofamericanscience.org. 10. doi:10.7537/marsjas140718.10.

Keywords: annealing temperature; corrosion; hexaluminate.

1. Introduction

Further advances in coating technology, over the past decades have resulted in its possible commercial exploitation in providing the necessary protection for materials in the oil and gas industries. Yttria-stabilized zirconia (YSZ) is the current industrial thermal barrier coatings materials (TBCs), which can long-term, operate at temperatures below 1100 ^{o}C. At higher temperatures, the phase transformation and accelerated sintering of YSZ tend to lead early spallation failure of TBC. Therefore, lower thermal conductivity, high thermal durability, and improved lifetime while considering the overall cost are still demanded in TBCs development especially for crude oil pipelines and during the refinement of the petroleum. Thermal barrier coatings (TBCs) are generally composed of a porous, insulating ceramic oxide top layer (yttria-stabilized zirconia (YSZ) is state of the art) which provides thermal protection, a thermally grown aluminum-rich oxide layer (TGO) which provides oxidation and hot corrosion protection, and an underlying aluminide (nickel or platinum) bond layer which is used to form the TGO layer (Clarke, 2003; Evans, 2008). For integration into the TBCs, materials require low thermal conductivity, a sufficiently high thermal expansion coefficient, phase stability up to temperatures higher than 1400 ^{o}C, stable pore morphology, and chemical and mechanical compatibility with the underlying layers. Lower thermal conductivity, high thermal durability, and improved lifetime while considering the overall cost are still demanded in TBCs development. It is therefore of great interest to compensate the loss in mechanical properties of zirconia-containing materials through the incorporation of other dispersions which can interact with the fracture and therefore maintain good toughness and, if possible, strength also at high temperatures (Pezzotti, 1993). The increase in thermal conductivity of coatings caused by densification due to increasing the operating temperature is an additional important issue which reveals the need for materials with low sinter ability at elevated temperatures. These materials should substitute YSZ for long-term high temperature applications due to the common problems with YSZ (e.g., dramatic aging at temperatures above 1100^{o}C and post sintering, which reduce the thermal conductivity). Since oxygen diffusivity of zirconia increases with temperature and leads to constant oxidation of the bond layer and consequently failure of the TBCs in operation, materials with lower oxygen diffusivity are required as well [Clarke, 2003; Azzopardi, 2004]. One of the main problems in developing this material as a thermal barrier coating is difficulty in controlling the microstructure in order to combine the low thermal conductivity with high structural reliability. The performances of ceramic materials are closely related to the ways they are processed. The conventional solid state reaction method requires high calcinations and sintering temperatures, resulting in a wide grain size distribution, multiple phases and inevitably some degree of porosity that worsening the micro-structural and subsequently the thermal properties of the materials. Therefore, the focus nowadays is on the synthesis of hexaluminate as promising materials for high temperature thermal barrier coatings. Magnesium hexaluminate and Lanthanum hexaluminate, abbreviated as MHA and LHA, respectively, with a

defective magnetoplumbite crystal structure and a plate-like grain structure have the potential to be applied as high temperature TBCs. Although the thermal conductivity of MHA and LHA (0.8–2.6Wm^{-1} K^{-1}) is to some extent higher than that of YSZ (0.6–2.3Wm^{-1} K^{-1}), however its low Young's modulus, low sinterability, superior structural and thermochemical stability up to 1400 ^{o}C, stable pore structure, lower oxygen diffusivity, and phase compatibility with Al_2O_3 as the TGO layer up to 1800^{o}C draw attentions to investigate LHA and MHA as a candidate for high temperature TBCs (Friedrich, 2001; Gadow, 2002; Cinibulk, 1995; Negahdari, 2010). The low thermal conductivity of these ceramics top layers is due to the defects and porosity which they introduce into the system. Poor intrinsic mechanical properties of LHA in addition to the presence of porosity could limit the structural reliability and fracture toughness of LHA-based TBCs (Negahdari, 2009). Hexaluminates has the magnetoplumbite crystal structure (Utsunomiya, 1988; Chandradass, 2009). In which the divalent metals occurs in cleavage planes located between blocks of Al_2O_3 spinel structure containing 20 octahedral Al per unit cell. The remaining two Al atoms per unit cell are associated with the cleavage plane, and are suggested to be in irregular five-coordinated environments. The behavior of Al in this phase during its structure evolution is therefore of interest for the unusual Al environment in both amorphous and crystalline aluminates. The materials' performances are closely related to the ways they are processed. Synthesis method of ceramic powders has played a significant role in determining the microstructure, thermal and mechanical properties of these ceramics materials (Hu, 2006; Yoshimura, 2008; Moon, 1999). Conventionally, these materials were produced by a conventional solid-state reaction of mechanically mixed oxides powders at high annealing temperatures (>1200 °C). This technique has some inherent disadvantages include chemical inhomogeneity, coarser particle size, and introduction of impurities during ball milling (Baba, 1972). The inevitable inhomogeneity that is inherent to this technique inhibits the required compositional and microstructural homogeneity of sintered products. Various wet chemical methods have been developed for the synthesis of nanocrystalline pure single-phase mixed-oxide powders including co-precipitation (Radwan, 2007), glass crystallization (Sato, 1993), self-propagating high-temperature synthesis method (Hu, 2010), hydrothermal method (Huo, 2009; Wang, 2010), mechanical alloying (Ding, 1998), and sol–gel method (Surig, 1994). Most of these methods are economically unfeasible for large scale production. One of the successful techniques for single-phase of nanocrystalline mixed oxide powders is the carboxylic acid process. By this method, a nanocrystalline powder with low-processing temperature and homogeneous microstructure, narrow size distribution and uniform shape can be produced. The process involves the ability of certain weak carboxylic acids (citric acid, oxalic acid or tartaric acid) to form chelates with several of cations in solution. These chelates can undergo polyesterification when heated to form a polymeric resin. The cations are, ideally, uniformly dispersed on an atomic scale throughout the polymeric resin. Further heating of the resin in air results in removal of all organics and the formation of a char having a controlled cation stoichiometry, with little segregation of the cations. The char is then heated to higher temperatures and oxidized to form the mixed-metal oxides. This method has been used to produce niobates, titanates, zirconates, chromates, ferrites, manganites, aluminates, cobaltites, and silicates (Eror, 1986; Lessing, 1989; Tai, 1992; Xu, 2005; Xu, 2005a; Yuan; 2007; Cao, 2005; Xu, 2000; Xu, 2005b). This study focused on two objectives: the first part wasto evaluate the performance of a proposed metallic coating at high temperature. The metallic coating involved in this project was selected to be used to coat a flare tip in an oil refinery. The second objective was developing and understanding the synthesis behavior of nanosized strontium hexaluminate, powders via organic carboxylic acid precursor methods. Tartaric acid was used as the source of the carboxylic acid. Organic acid precursor method is used to form uniform very small nano-sized powders, homogenous particles and good morphology. Moreover, the produced hexaluminates can be tested as thermal barrier coating under high temperature conditions and reducing gases.

2. Material and Methods

The first objective of the experimental work was to evaluate the performance of prepared samples coated with conventional thermal barrier material. Then, developing a practical method to produce hexaluminate powder as a candidate coating material at high temperature. In the first experiment, coated samples made of SS310 were utilized to evaluate the proposed coating system which has the following characterizations: a bond coat: AMDRY 995M using plasma equipment (Co32Ni21Cr8Al0.5Y), thermal barrier: Metco 204-NS Yttria-stabilized-zirconia powder. This is a spherical, free flowing, partially stabilized, 7-8 % Yttria zirconia Powder manufactured by Metco. In order to simulate the real environment in the field, several different gases were introduced to the experiment and the operating temperature was set at ≥ 1000 ^{o}C. Several gases were used in this study such as SO_2, H_2S, H_2, CO and CO_2 both as single gas

or mixture of gases. The experimental apparatus and measuring system used in this study are shown in Fig. 1. The furnace is a vertical one equipped with nickel chrome heating elements and controlled by a SCR power regulator. Reaction tube (60 mm I.D. and 800 mm L.) was made of fused silica and mounted in the furnace. The oxidizing gas was prepared by mixing the gas components, whose flow rates were precisely controlled by the respective digital thermal mass flow controllers (MFG).

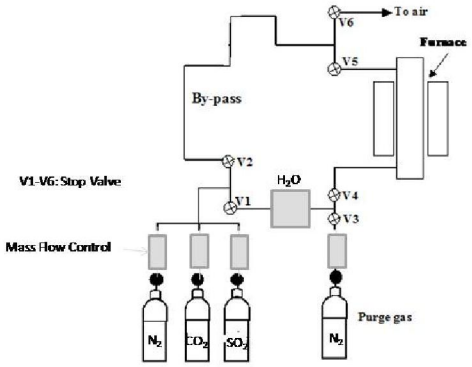

Figure 1. Schematic of gas line and valve system

The second part of the experimental work was a new methodology for the synthesis of a hexaluminat powder material. A tartrate precursor method was applied for the preparation of aluminum-strontium tartarte precursor for the synthesis of $SrA1_{12}O_{19}$. Tartaric acid precursor technique was involved at the preparation of aqueous solution of the required cation, the chelation of cations in solution by addition of tartaric acid then, raising the temperature of the solution until formation the precursor. The precursor was calcined at low temperature compared by other methods to form the powders. The tartaric acid was not only used to form stable complexes with starting metallic ions, but also it was used as organic rich fuel. The process is very simple and available for most of piezoelectric materials. Pure chemical grade of Aluminum nitrate, Strontium carbonate, in the presence of stoichiometric amount of tartaric acid were used as starting materials. The mixture of Sr-Al, solution was firstly prepared and then stirred for 15 minute on hot plate magnetic stirrer, followed with addition of an aqueous solution of tartaric acid to the mixture with stirring. Then, the solution was evaporated to 80 ^{o}C with constant stirring until dryness and then dried in a dryer at 100^{o}C overnight. The dried powders obtained as aluminates precursors. Thermal analysis of the un-annealed precursors was carried.

3. Results and Discussions

A typical thermal barrier coat (TBC) microstructure is shown in Fig (2). The blank sample composed of two coating layers the outer one is the ceramic layer of the TBC and the inner one is the bond coat, in addition to the substrate alloy. Some position shows good adhesion between the zirconia layer and the bond coat and no cracks are detected Fig (3).

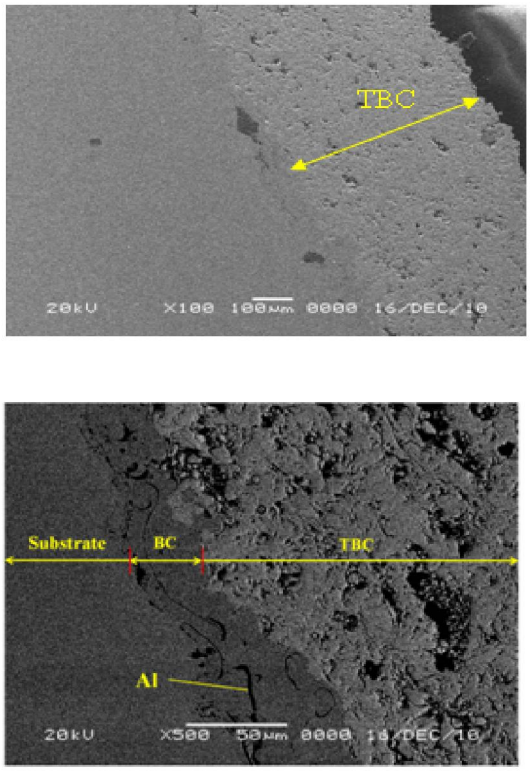

Figure 2. SEM image of blank sample showing two coating layers

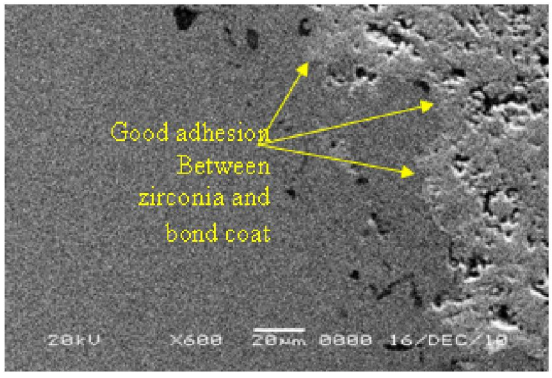

Figure 3. SEM image shows different degrees of adhesions at the BC and TBC interface.

The coated sample was exposed to the corrosion atmosphere at 975 °C for two days. Generally, it suffered serious corrosion at one surface while the opposite surface was good Fig (4).

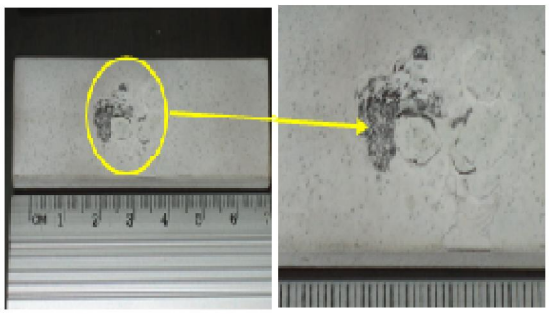

Figure 4. Visual inspection of zirconia coating after exposure for 2 days.

On the other hand, many cracks were observed with different lengths and diameters in zirconia layer and at the interface between zirconia layer and bond coat layer. The serious cracks were concentrated near the interface between zirconia layer and bond coat layer. This reflects the bad adhesion between the bond coat and zirconia at these positions. The presence of cavities beneath the ceramic layer was very serious. Generally, the TBC layer has weak microstructure which has many crack and cavities. In the position where there is good adhesion between zirconia layer and bond coat, usually cracks were noticed at the interface and part of zirconia adhesive to the bond coat was pulled out the zirconia matrix.

Corrosion product (oxides) of the bond coat layer and substrate alloy swell due to the capture of oxygen (oxide grains is much bigger than metallic grains) and made mechanical stress on the zirconia layer. This initiated broad cracks in TBC layer due to its weak structure, Fig. (5).

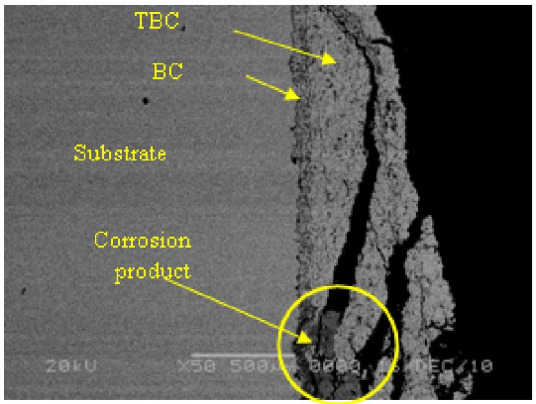

Figure 5: SEM image shows inclusion of the corrosion product into the TBC layer.

The second part focused on the preparation of strontium hexaluminate from the precursor containing strontium - aluminum tartrate, as candidate material for TBC. Thermal analysis (TG-DTG-DSC) for uncalcined precursors was carried out. The profile illustrated the steps of the thermal decomposition of the tartarate mixtures. The rate of heating kept at 10°C/min between room temperature and 1200°C. The measurements were carried out in a current of nitrogen atmosphere. Fig. (6) Illustrates the profiles of thermal analysis (TG), differential thermal analysis (DTG) and differential scanning calorimetry (DSC) of the parent sample during the decomposition of the strontium - aluminum tartrate precursors at a heating rate of 10°Cmin^{-1} in nitrogen atmosphere. The first and second decomposition steps started with a small weight loss 1.74% and 4.88% at 130 and 177°C, respectively, assigned to the moisture content that still from the sample. As the temperature increase between 200 to 580°C (DSC = 400°C), rapid and major weight loss of dropped in a weight loss according to the decomposition of tartrate precursor. The sample undergoes exothermic multistep weight loss between 177 °C and 580 °C due to the decomposition of carbonaceous mass of the tartrate precursor. This weight loss was reflected as broad exothermic peaks in DSC curve at around 400 °C. The sample weight seemed to be constant after the temperature reach to 580°C. However, the total mass loss was about 58.7% at 580 °C. Beyond 585 °C, there was no significant weight loss until 1200 °C.

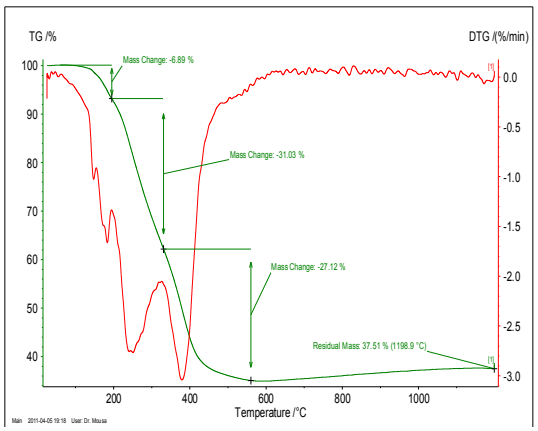

Figure 6: Thermo-gravimetric analysis for Strontium-aluminate tartrate precursor.

SEM examinations of the synthesized powders (Fig. 7) revealed that they were essentially, slack and porous crystals, and have many holes. The grains did not look plate- like crystals, and that is because of the short time of annealing. Moreover, the powders have a

particles size of 10-25 µm. This result together with other analysis using thermal analysis, support the proposed method for synthesizing oxide with magnetoplumbite structure of the general composition, $SrA1_{12}O_{19}$ via tartaric acid has been successfully obtained.

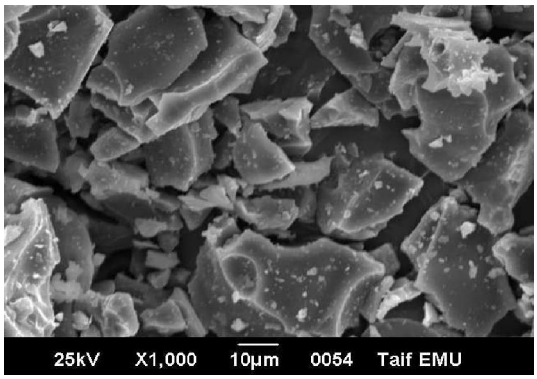

Figure 7: SEM microstructure of SrAl12O19 prepared at 1300 for 2 h.

4. Conclusion

1. Despite the beneficial effect of the thermal barrier coating (TBC) in protecting the alloy SS310 from corrosion for some time, it actually had failed on the resistant to corrosive environment for long period of exposure.

2. TBC layer porosity should be lowered to fall in the range of 10-15 µm. typically; finer particle size and closer spray distance results in lower porosity.

3. The use of tartaric acid gel method has facilitated the crystallization of $SrAl_{12}O_{19}$ at relatively low temperatures.

4. It is recommended that further work should be carried out to provide more information on the synthesis of $SrAl_{12}O_{19,}$ and other hexaluminates compounds to be used as a TBC materials.

Corresponding Author:
Materials and Corrosion Group
Department of Chemistry
Taif University, Saudi Arabia
E-mail: mohsen9907@hotmail.com

References

1. D.R. Clarke, C.G. Levi. Material design for the next generation of thermal barrier coating. Annu Rev Mater Res 33 (2003) 383.
2. A.G. Evans, D.R. Clarke, C.G. Levi, J. Eur. Ceram. Soc. 28 (2008) 1405.
3. G. Pezzotti, Acta. Metall. Mater., 41 (1993) 1825.
4. A. Azzopardi, R. Mevrel, B.S. Ramond, E. Olson, K. Stiller, Surf. Coat. Technol131 (2004) 177.
5. C. Friedrich, R. Gadow, T. Schirmer, J. Therm. Spray. Technol10(4) (2001) 592.
6. R. Gadow, M. Lischka, Surf. Coat. Technol151 (2002) 392.
7. M.K. Cinibulk, J. Mater. Sci. Lett. 14 (1995) 651.
8. Z. Negahdari, M. Willert-Porada, F. Scherm, J. Eur. Ceram. Soc. 30 (2010) 3103.
9. Z. Negahdari, M. Willert-Porada, Adv. Eng. Mater. 11, 12 (2009) 1034.
10. A. Utsunomiya, K. Tanaka, H. Morikawa, F. Marumo, H. kojima, J. Solid State Chem. 75 (1988) 197.
11. J. Chandradass, D. S. Bae, K. H. Kim, J. Non-Crystalline Solids, 355 (2009) 2429.
12. Y.M. Hu, H.S. Gu, X.C. Sun, J. You and J. Wang, Appl. Phys. Lett.88 (2006), 193.
13. M. Yoshimura, K. Byrappa, J. Mater. Sci.43, 7 (2008), 2085.
14. J. Moon, M.L. Carasso, H.G. Krarup, J.A. Kerchner and J.H. Adair, J. Mater. Res.14, 3 (1999), 866.
15. P. D. Baba, G.M. Argentina, W.E. Courtney, G.F. Dionne and D.H. Temme, IEEE Trans. Mag. 8 (1972) 83-94.
16. M. Radwan, M.M. Rashad and M.M. Hessien, J. Mater. Process. Technol. 181(2007) 106.
17. H. Sato and T. Umeda, J. Mater. Trans.34 (1993) 76.
18. P. Hu, H. Yang, D. Pan, H. Wang, J. Tian, S. Zhang, X. Wang, A. A. Volinsky, J. Magn. Magn. Mater. 322 (2010) 173.
19. J. Huo, M. Wei, Mater. Lett. 63 (2009) 1183.
20. L. Wang, J. Ren, Y. Wang, X. Liu, Y. Wang, J. Alloy. Compd. 490 (2010) 656.
21. J. Ding, W.F. Miao, R. Street, P.G. McCormick, R. Street, J. Alloys Compd. 281(1998) 32.
22. C. Surig, K.A. Hempe, D. Bonnenborg, J. IEEE Trans. Magn. 30 (1994) 4092.
23. N.G. Eror, H.U. Anderson, in: C.J. Brinker, D.E. Clark, D.R. Ulrich (Eds.), Proceedings of the Materials Research Society Symposium on Better Ceramics Through Chemistry II, Palo Alto, CA, April, Materials Research Society, Pittsburgh, PA, 1986, p. 571.
24. P.A. Lessing, Am. Ceram. Soc. Bull. 68 (1989) 1002.
25. L.W. Tai, P.A. Lessing, J. Mater. Res. 7 (1992) 502.
26. Y.B. Xu, X. Yuan, G.H. Huang, H. Long, Mater. Chem. Phys. 90 (2005) 333.

27. Y.B. Xu, P.X. Lu, G.H. Huang, C.L. Zeng, Mater. Chem. Phys. 92 (2005) 220.
28. X. Yuan, Y. B. Xu, Y. He, Mater. Scienc. Engin. A, 25 (2007) 142.
29. W. Cao, Y.B. Xu, S.J. Wang, P.X. Lu, G.H. Huang, C.F. Xu, Mater. Lett. 59 (2005) 1914.
30. Y.B. Xu, X.M. Chen, Y.J. Wu, J. Mater. Sci. Mater. Electron. 11 (2000) 633.
31. Y. Xu, W. Peng, S. Wang, X. Xiang, P. Lu, Mater. Scienc. Engin. B 123 (2005).

7/25/2018